American Mineralogist, Volume 62, pages 51–59, 1977

Gerstmannite, a new zinc silicate mineral and a novel cubic close-packed oxide structure

PAUL B. MOORE AND TAKAHARU ARAKI

Department of the Geophysical Sciences
The University of Chicago, Chicago, Illinois 60637

Abstract

Gerstmannite, $(Mn,Mg)Mg(OH)_2[ZnSiO_4]$, orthorhombic, a 8.185(7), b 18.65(2), c 6.256(6)Å, $Z = 8$, space group *Bbcm*, occurs as white to pale-pink mats and sprays of bunched prismatic crystals associated with calcite, manganpyrosmalite, and sphalerite in a hydrothermal vein paragenesis which cuts normal franklinite–willemite "buckshot" ore from the Sterling Hill Mine, Ogdensburg, Sussex County, New Jersey. Hardness = 4½; sp gr = 3.68(2) [3.66 g cm^{-3} calculated for $(Mg_{0.625}Mn_{0.375})_2Zn(OH)_2(SiO_4)$]; cleavage good parallel to {010}. The prisms are composed of {100}, {010} and {110} with no terminations. Biaxial (−), α 1.665(2), β 1.675(2), γ 1.678(2), $2V \sim 50$–60°, $X \| b$, $Y \| c$, $Z \| a$.

$R = 0.042$ for 1091 independent reflections. The structure is based on oxygen cubic close-packing, the close-packed layers parallel to {130}. The structure is comprised of $^2_\infty[MnMgO_3(OH)_2]$ octahedral sheets linked to $^2_\infty[ZnSiO_4]$ tetrahedral sheets which are parallel to {010}. Average bond distances are $^{[6]}Mn$–$^{[3.5]}O = 2.21$Å, $^{[6]}Mg$–$^{[3.7]}O = 2.08$Å, $^{[4]}Zn$–$^{[3]}O = 1.95$Å and $^{[4]}Si$–$^{[3.3]}O = 1.64$Å, where the left superscripts refer to the average coordination numbers of the atoms involved.

Introduction

During the summer of 1975, Mr. Ewald Gerstmann of Franklin, New Jersey, brought to the senior author's attention two fist-sized samples of a curious pink prismatic mineral constituting the greater fraction of a well-layered vein cutting normal franklinite–willemite ore. According to Mr. John L. Baum (personal communication), the samples were gathered about five years ago, but the peculiar nature of the mineral was not then recognized, and but few specimens were preserved. The material originated from the 1120′ stope above the 1100′ level in the Sterling Hill Mine, Ogdensburg, Sussex County, New Jersey. More specifically, it occurred in the "west vein," just north of the east branch of that vein. Quoting Mr. Baum, "The ore was a pale banded willemite–franklinite compact ore, more yellow than green and certainly not red or brown, with secondary willemite veinlets containing in this case the unknown. The vein wall-rock is white marble. The vein generally shows some zincite on its footwall and some black willemite on its hanging wall." Preserved specimens include one fragment at the Smithsonian Institution, one at Harvard University, two in the collection of Mr. Baum, two preserved by Mr. Nick Zipco (Franklin, New Jersey), one by Mr. Steve Sandford (Franklin), and two in the collection of Mr. Gerstmann (cotype and paratype). There is some evidence that other specimens have been dispersed to buyers of mineral specimens.

The type specimen shows ore consisting of "buckshot" franklinite and pale flesh-pink to yellowish willemite in equal amount dispersed through a gangue of manganoan calcite. The ore mineral grains range from 1 mm to 3 mm in diameter and comprise about half the volume of the rock. The vein sharply cuts the ore and is clearly well-layered. The base is comprised of a thin layer of magnesian calcite upon which was deposited a mixture of waxy brown manganpyrosmalite and yellow-brown lustrous cleavage surfaces of sphalerite. Upon these minerals rest calcite and the new mineral, hereafter named gerstmannite, the thicker portions of the latter ranging up to 3 cm. Occasional solution cavities dot the gerstmannite within which minor amounts of unidentified species reside.

Mr. Gerstmann's second specimen, the paratype in this study, affords sufficient information to establish the new mineral's paragenesis. It measures about 7 × 9 × 5 cm and consists of a thick vein, the greater portion of which is translucent apple-green willemite

exhibiting bright-green fluorescence and dull-green phosphorescence under short-wave ultraviolet excitation. Gerstmannite occurs in generous amount on one side of the vein as coarse rosettes of pale-pink crystals. It is not fluorescent under short- or long-wave ultraviolet excitation. Remnant grains of a bright pink mineral occur embedded in the adjacent willemite and exhibit partial replacement by the new mineral. Single-crystal study established the pink mineral as alleghanyite. Dr. Brian Mason kindly communicated an uncorrected electron probe analysis which afforded $K_2O < 0.1$, $CaO < 0.1$, MnO 48.2, FeO 0.2, MgO 14.8, ZnO 3.6, $Al_2O_3 < 0.1$, SiO_2 26.7 percent or approximately $(Mn_{0.62}Mg_{0.34}Zn_{0.04})_5(SiO_4)_2(OH)_2$, a magnesian alleghanyite. Remnant brown patches of superficially oxidized pyrochroite were also noted in the vein.

The paragenesis, not unusual for the Sterling Hill deposit, is interpreted as a hydrothermal vein assemblage formed at moderate temperature under basic and reducing conditions. The gerstmannite is the latest product in the sequence as it replaces the willemite, alleghanyite, and pyrochroite. Setting M^{2+} = octahedral cations, a univariant reaction can be written, *viz*:

$$\underset{\text{pyrochroite}}{3M^{2+}(OH)_2} + \underset{\text{alleghanyite}}{M_5^{2+}(OH)_2(SiO_4)_2} + \underset{\text{willemite}}{2Zn_2SiO_4} \rightarrow \underset{\text{gerstmannite}}{4M_2^{2+}(OH)_2(ZnSiO_4)},$$

accepting as the components $M(OH)_2$, M_2SiO_4, and Zn_2SiO_4. When establishing the amount of each phase participating in the equation, it is more convenient to determine its ratio based on oxygen, since the structures are all close-packed. The ratio of the reactants is 3:5:4 with respect to oxygen and suggests that the greater portion of alleghanyite in the vein was destroyed in the formation of the gerstmannite. A similar reaction can be written for other manganese humites, for example

$$\underset{\text{pyrochroite}}{M(OH)_2} + \underset{\text{"Mn–norbergite"}}{M_3(OH)_2(SiO_4)} + \underset{\text{willemite}}{Zn_2SiO_4} \rightarrow \underset{\text{gerstmannite}}{2M_2(OH)_2(ZnSiO_4)}$$

The model is admittedly simple since the phases involving (Mn,Mg) solution are probably substantially ordered with respect to these cations. We shall provide evidence that Mn and Mg are ordered in the gerstmannite structure, but no results are as yet available for the degree of Mn and Mg ordering in the humite structures. The simple model suggests, however, that gerstmannite is confined to a basic hydrothermal vein assemblage where pyrochroite, willemite, and a manganese humite are present.

Description and properties

Physical properties

Gerstmannite is translucent to opaque, and white to palest pink in color. The streak is white. The luster is vitreous to subadamantine along cleavage surfaces, although thick mats tend to exhibit a silky appearance. The species occurs as mats and sprays of bunched prismatic crystals, the individuals measuring up to 2 × 2 × 10 mm. Individuals are not terminated, but consist of well-developed prisms including {100}, {010}, and {110}. The hardness is 4½ on Mohs scale, specific gravity 3.68(2) determined on the Berman torsion balance (T = 21.0°C), with toluene as the displaced fluid. The density, calculated from $(Mg_{0.625}Mn_{0.375})_2Zn(OH)_2(SiO_4)$ and the structure cell criteria, is 3.66 g cm^{-3}. The cleavage is good parallel to {010}.

Specimens of gerstmannite closely resemble pectolite, miserite, thomsonite, and scoecite in appearance. The indices of refraction, which are much higher for gerstmannite than these other species, are perhaps the most reliable simple means of identification. The mineral dissolves slowly in dilute HCl solution at room temperature, and the solution is clear and colorless.

X-ray crystallography

Powder, single-crystal rotation, Weissenberg, and precession photographs were obtained. In addition, a powder diffractogram (Cu$K\alpha$ radiation, graphite monochromator, chart speed ½° min^{-1}, corrections for absorption, sample shape, and chart setting) was obtained and completely indexed (Table 1). Least-squares refinement of these data led to a 8.185(7)Å, b 18.65(2)Å, c 6.256(6)Å, within the limits of error for measurements on calibrated precession films utilizing Mo$K\alpha$ radiation [a 8.176(7)Å, b 18.65(1)Å, c 6.251(5)Å]. The success of a detailed three-dimensional crystal structure analysis and the single crystal studies force us to conclude that the space group is orthorhombic *Bbcm*.

A structure analysis affords the opportunity for obtaining a calculated powder pattern, the results of which appear in Table 1. There are definite advantages in calculating such a pattern, since unambiguous Miller indices are obtained and effects such as preferred orientation can be assessed. Taking this into account, the agreement between calculated and observed data is good.

It is noted that gerstmannite possesses a good {010} cleavage, since the observed reflections of the type ($0k0$) are enhanced.

Table 1. Gerstmannite. Observed and calculated powder data†

I(obs)	I(calc)	d(obs)	d(calc)	hkl	I(obs)	I(calc)	d(obs)	d(calc)	hkl
85	49*	9.326	9.325	020	20	24	1.9982	1.9986	420
50	38	4.806	4.803	111		3		1.9436	430
25	10*	4.661	4.663	040		3		1.9219	133
40	23	4.388	4.386	121	35	15*	1.9124	1.9127	191
10	11	4.088	4.092	200		4		1.8737	440
15	19	3.994	3.997	210	25	13	1.8692	1.8693	082
5	2	3.881	3.882	131		3		1.8488	290
15	14	3.747	3.747	220	10	11	1.8168	1.8174	272
80	62	3.418	3.418	230	5	6	1.7763	1.7769	153
	16		3.401	141		4		1.7124	402
20	7*	3.108	3.108	060	5	3	1.7053	1.7053	381
20	14	3.078	3.076	240	5	4	1.7001	1.7003	282
60	29	2.983	2.983	151	5	7	1.6842	1.6842	422
	16		2.966	022		4		1.6509	432
75	58	2.758	2.757	250	5	5	1.6502	1.6504	313
100	100	2.598	2.598	042		4		1.6019	0.10.2
	7		2.485	202	10	6	1.6010	1.6010	333
25	19	2.480	2.479	311	10	11	1.5912	1.5916	292
50	43	2.466	2.464	212		3		1.5780	511
25	20	2.403	2.401	222	25	21	1.5644	1.5641	004
10	4	2.348	2.348	171		8		1.5562	452
75	17*	2.332	2.331	080	45	10*	1.5548	1.5542	0.12.0
	5		2.320	331		3		1.5142	353
15	16	2.308	2.308	232	35	47	1.5002	1.4999	462
30	19	2.232	2.233	270	10	12	1.4920	1.4917	2.10.2
10	5	2.204	2.205	062	5	5	1.4403	1.4405	472
5	6	2.193	2.193	242	5	7	1.4223	1.4223	234
10	11	2.076	2.077	351	5	7	1.4003	1.4006	2.11.2
	9		2.068	252	10	5	1.3920	1.3919	0.12.2
5	5	2.046	2.046	400	15	10	1.3787	1.3784	4.10.0
10	5	2.025	2.026	280	10	9	1.3603	1.3604	254
	4		2.009	113					

† $CuK\alpha$ radiation, graphite monochromator, 0.5° min^{-1} in 2θ. The data were corrected for absorption and sample shape (two variable parameters). Peak heights were measured. Reflections enhanced by preferred orientation are starred.

Chemical composition

The results of one wet-chemical analysis, one determination of water (by Penfield tube), and one electron probe analysis are summarized in Table 2. All material was gathered from the type specimen. Dr. Jun Ito informed us that emission spectrographic analysis revealed trace quantities of Ti, Ag, Al, Cu, Cd(?), and As(?). The original batch of separated crystals was known to contain some calcite, estimated to be 3.93 percent by weight. Since Ca was not detected in the probe analysis, its amount determined the calcite present. A qualitative probe scan revealed that the calcite contained only minor amounts of Mg, Mn, and Zn. Dr. A. J. Irving informed us that the probe grain was homogeneous throughout. Standards included synthetic diopside (Mg,Si), Minas Gerais rhodonite (Mn), and Franklin, New Jersey, willemite (Zn), the last a fragment of material analyzed by the late L. H. Bauer. No other elements between Na and U were detected.

The composition for gerstmannite is close to $Mn_{0.75}Mg_{1.25}Zn(OH)_2(SiO_4)$. The crystal structure analysis converged close to this composition, revealing $Mn_{0.79}Mg_{1.21}Zn(OH)_2(SiO_4)$. That study also established a highly ordered structure from which the formula $(Mn,Mg)MgZn(OH)_2(SiO_4)$ is proposed. Thus, the type gerstmannite is magnesian, its ideal end-member composition being $MnMgZn(OH)_2(SiO_4)$.

Although gerstmannite compositionally resembles hodgkinsonite, $^{[6]}Mn^{[4]}(Zn_2Si)O_4(OH)_2$, a rather abundant vein mineral from the abandoned Franklin deposits nearby, the structure analysis reveals a new structure type based on cubic close-packed oxygens. We propose that the mineral be classed with staurolite, kyanite, and $Mg_4O[Si_2O_7]$ ("β–spinel") owing to the principle of cubic close-packing.

Optical properties

Gerstmannite is biaxial (−), α 1.665(2), β 1.675(2), γ 1.678(2), $2V \sim 50$–60° (observed), $X||b$, $Y||c$, $Z||a$.

Table 2. Gerstmannite. Chemical analyses

	1	2	3	4	5
Na_2O	0.04	0.04	nil	-	-
CaO	2.2	-	nil	-	-
MgO	16.0	16.6	19.5	-	19.2
MnO	21.2	22.1	21.1	-	20.2
FeO	0.06	0.06	nil	-	-
ZnO	30.5	31.7	29.6	-	30.9
SiO_2	23.0	23.9	23.2	-	22.8
H_2O	n.d.	n.d.	n.d.	4.12	6.9
		94.4	93.4		100.0

[1]J. Ito, analyst, on 90 mg. sample. The presence of calcite was detected. Emission spectrographic analysis revealed trace quantities of F, Ti, Ag, Al, Cu, Cd?, As?.

[2]From (1), after deducting 3.93% $CaCO_3$ (calcite).

[3]A. J. Irving, analyst. By electron probe.

[4]J. Ito, analyst, on 121.0 mg. sample, by Penfield tube.

[5]Computed for composition $(Mg_{0.625}Mn_{0.375})_2Zn(OH)_2(SiO_4)$.

The mineral is not discernably pleochroic. The calculated mean refractive index is 1.714, adopting the formula and density in this study and the specific refractive energies of Larsen and Berman (1934).

Name

It is a pleasure to christen the new species in honor of Mr. Ewald Gerstmann from Franklin, New Jersey, who first brought the material to the senior author's attention. Mr. Gerstmann has preserved some of the finest specimens of nearly every species from these famous zinc deposits, and his private museum has been one of the centers of activity for those who journey to the Franklin–Ogdensburg mineralogical mecca.

The new species and name have received prior approval from the International Commission on New Minerals and New Mineral Names, International Mineralogical Association. The type specimen is preserved in the National Museum of Natural History, Smithsonian Institution and a cotype in the private collection of Mr. Gerstmann.

Crystal structure

Experimental

A single crystal of the type material measuring 0.13 mm ($||a$), 0.14 mm ($||b$), and 0.30 mm ($||c$) was mounted with its c axis parallel to the rotation axis of a *Pailred* diffractometer. With graphite monochromatized Mo$K\alpha$ (λ = 0.7093Å) radiation, automated full scan widths ranging from 2.4° to 6.4°, 2θ scan of 1° min^{-1}, reflections of (hkl) and $(h\bar{k}l)$ were collected up to $\sin\theta/\lambda = 0.80$ and the levels $l = 0$ through $l = 9$. Reflections where I_0 were unobserved were set $I_0 = 2\sigma I_0$. Several low-angle reflections within the blind region of the machine were manually scanned. The crystal shape, which was described by seven faces, was corrected for anisotropy in absorption by the Gaussian integration method (Burnham, 1966). Symmetry equivalent reflections were then averaged to yield 1091 independent reflections. Individual reflections were assigned weights based on long-term fluctuations of source intensity and counting statistics.

Solution and refinement of the structure

A full Patterson synthesis, $P(uvw)$, confirmed the suspicion that the structure was based on oxygen dense-packing, the layers stacked parallel to the {130} plane. Search for octahedral and tetrahedral occupancies which satisfied the interatomic vector set provided cations and anions as trial input for β synthesis (Ramachandran and Srinivasan, 1970). A final γ' synthesis sufficiently sharpened all positions so that least-squares refinement could be inaugurated.

Refinement proceeded from scattering factors for Mn^{2+}, Mg^{2+}, Zn^{2+}, Si^{4+}, and O^{1-} from Cromer and Mann (1968), anomalous dispersion corrections, f'',

Table 3. Gerstmannite. Atomic coordinate parameters*

			x	y	z
Mn†	8	m	0.00721(8)	0.39594(4)	$\frac{1}{2}$
Mg	8	$\bar{1}$	$\frac{1}{4}$	$\frac{1}{2}$	$\frac{1}{4}$
Zn	8	2	.40033(6)	$\frac{1}{4}$	$\frac{1}{4}$
Si	8	m	.14422(12)	.34580(5)	0
OH(1)	8	2	0	$\frac{1}{2}$	0.2822(5)
OH(2)	8	m	.2501(4)	.4306(1)	$\frac{1}{2}$
O(1)	8	m	.2484(4)	.4205(1)	0
O(2)	8	m	.2775(4)	.2793(1)	0
O(3)	16	1	.0294(3)	.3373(1)	.2112(3)

*Estimated standard errors refer to the last digit. Included in the list are the equivalent point rank numbers and the point symmetries.

†Refined to 0.786(9)Mn + 0.214Mg.

Table 4. Gerstmannite. Anisotropic thermal vibration parameters ($\times 10^4$)*

	β_{11}	β_{22}	β_{33}	β_{12}	β_{13}	β_{23}
Mn	28.8(11)	6.2(2)	47.4(19)	0.0(2)	0	0
Mg	43.9(21)	4.9(3)	48.2(32)	0.1(7)	-10.7(16)	0.9(5)
Zn	39.6(9)	4.7(2)	43.7(16)	0	0	0.9(1)
Si	27.4(14)	3.9(3)	45.2(22)	-0.6(4)	0	0
OH(1)	19.2(31)	5.2(6)	62.0(53)	0.9(10)	0	0
OH(2)	42.4(33)	5.7(6)	39.4(43)	-0.9(12)	0	0
O(1)	36.7(31)	2.8(5)	59.2(47)	-2.9(10)	0	0
O(2)	43.0(34)	6.3(6)	48.3(44)	9.2(11)	0	0
O(3)	41.2(24)	5.0(4)	71.1(40)	-1.4(8)	21.3(26)	-3.5(11)

*Coefficients in the expression $\exp-[\beta_{11}h^2 + \beta_{22}k^2 + \beta_{33}\ell^2 + 2\beta_{12}hk + 2\beta_{13}h\ell + 2\beta_{23}k\ell]$.

from Cromer and Liberman (1970), and refinement for the coefficient for secondary extinction (Zachariasen, 1968). The chemical analysis suggested that (Mn,Mg) solid solution may exist in the crystal, and of the two independent octahedral sites, one afforded pure Mg^{2+} and the other exhibited (Mn,Mg) solution. The site distribution for the latter position was assessed by a local modification of a least-squares program reported by Finger (1968). The final cycle included as variable parameters one scale factor, one coefficient of secondary extinction, one site population parameter, fifteen atomic coordinate parameters, and forty anisotropic thermal vibration parameters. The final cycle led to $R = (\Sigma||F_o| - |F_c||)/(\Sigma|F_o|) = 0.042$ for all 1091 independent reflections and 0.033 ($Rw = 0.049$) for those non-zero 766 reflections, with $w = \sigma^{-2}$ of $|F_o|$. Refinement minimized $\Sigma w(F_o - F_c)^2$. The secondary extinction coefficient, c_o, is $0.59(19) \times 10^{-6}$ and the overall scale factor, s, is 2.13(1). The goodness-of-fit $\Sigma w(F_o - F_c)^2/\Sigma(n - m)$, where n = number of independent data and m = number of parameters = 0.709.

The success of the refinement requires that Mg^{2+} completely occupy the inversion center at (¼ ½ ¼), *etc.*, and that the octahedral population on the mirror plane is in fact $0.786(9)Mn^{2+} + 0.214Mg^{2+}$. This is further substantiated by the excellent convergence in thermal vibration parameters to expected values; and the chemical analyses, whose average suggests $0.75Mn^{2+} + 0.25Mg^{2+}$. Thus, type gerstmannite is a magnesian variant of the ideal composition $MnMgZn(OH)_2(SiO_4)$. Atomic coordinate parame-

Table 5. Gerstmannite. Parameters for the ellipsoids of vibration*

Atom	i	μ_i	θ_{ia}	θ_{ib}	θ_{ic}	B(Å^2)	Atom	i	μ_i	θ_{ia}	θ_{ib}	θ_{ic}	B(Å^2)
Mn	1	.097(2)	90	90	0	.79(2)	OH(2)	1	.088(5)	90	90	0	.85(4)
	2	.099(2)	179	89	90			2	.100(6)	99	171	90	
	3	.104(2)	89	1	90			3	.120(5)	9	99	90	
Mg	1	.089(5)	72	127	43	.87(3)	O(1)	1	.065(6)	74	15	90	.77(3)
	2	.095(6)	105	143	123			2	.108(11)	90	90	180	
	3	.127(3)	157	89	67			3	.114(11)	15	105	90	
Zn	1	0.089(1)	90	144	54	0.80(2)	O(2)	1	.075(5)	52	142	90	.93(4)
	2	.095(1)	90	126	144			2	.098(8)	90	90	180	
	3	.116(1)	0	90	90			3	.142(6)	38	52	90	
Si	1	.082(3)	79	11	90	.66(2)	O(3)	1	.088(19)	111	42	56	.97(3)
	2	.095(7)	90	90	180			2	.095(23)	51	50	116	
	3	.097(7)	11	101	90			3	.141(5)	47	101	45	
OH(1)	1	.080(6)	13	103	90	.74(4)							
	2	.097(5)	103	167	90								
	3	.111(5)	90	90	0								

*i = ith principal axis; μ_i = r.m.s. amplitude; θ_{ia}, θ_{ib}, θ_{ic} = angles between ith principal axis and the cell axes, a, b and c. Estimated standard errors refer to the last digit. The equivalent isotropic thermal vibration parameter (B) is also listed.

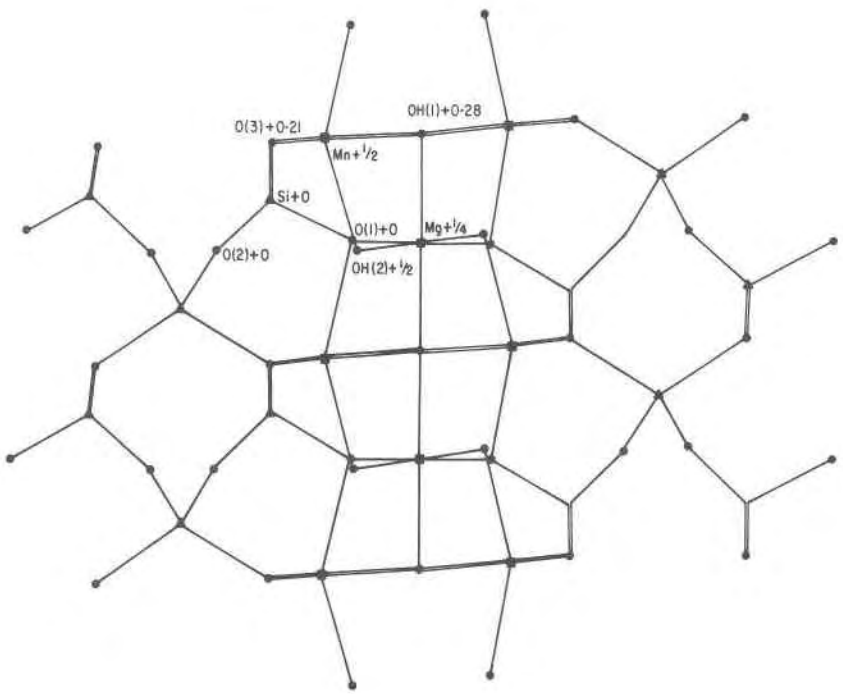

Fig. 1. Spoke diagram of the gerstmannite structure down [001]. The atoms are labelled to conform with Table 3. Note the distortions of the Mn–O and Mg–O octahedra.

ters appear in Table 3, anisotropic thermal vibration parameters in Table 4, the root mean square displacements of these parameters and their orientations in Table 5, and the structure factor list in Table 6.[1]

Description of the structure

Gerstmannite is an elegant example of a new kind of structure type based on oxygen cubic close-packing. The cell is metrically the same as that of manganostibite, $4^{[6]}(Mn_5Sb)^{[4]}(Mn_2As)O_{12}$, a 8.73Å, b 18.85Å c 6.06Å, *Ibmm*. Both structures possess 48 oxygens in the cell, the maximum allowable in a close-packed cell of this volume and shape, and the close-packed layers are stacked parallel to {130}. A diagram of the structure is shown in Figure 1. It is more convenient, however, to discuss the *ideal* arrangement which is based on perfect octahedra and tetrahedra. To achieve this, appropriate shading affords a diagram (Fig. 2) which can be compared with similar diagrams for other cubic close-packed oxide arrangements discussed by Moore and Smith (1970). This ideal arrangement, which does not discriminate among the kinds of atoms present but only whether the sites are occupied or not, has the same space group as the real structure. It is immediately seen that gerstmannite can be described as the linkage of octahedral (M) and tetrahedral (T) sheets which are oriented parallel to {010}. The octahedral sheets have formal composition $^{2}_{\infty}[MnMgO_3(OH)_2]$ and represent a slice of the NaCl structure along {110}. In this slice, the central MgO_6 octahedra link to form edge-sharing chains which run parallel to [001]. The lateral MnO_6 octahedra link by edge-sharing above and below to the MgO_6 octahedra, and link each other at a common edge to form a dimeric arrangement along [010]. Unlike NaCl, however, alternate levels of octahedral positions along [001] are empty (in NaCl the slab would have formal composition $M_3\phi_5$). The octahedral sheet is featured as an ideal arrangement down [010] in Figure 3a. Tetrahedral sheets of composition $^{2}_{\infty}[ZnSiO_4]$ link two octahedral sheets together to form a framework. The idealized sheets (Fig. 3b) exploit cubic close-packing through voids at alternate levels along [001] for the Si positions (in c.c.p., the tetrahedral slab would have formal composition $T_3\phi_4$). These observations compel us to conclude that gerstmannite is a zincosilicate whose formula should be written $MnMg(OH)_2[ZnSiO_4]$.

[1] To obtain a copy of this table, order Document AM-76-029 from the Business Office, Mineralogical Society of America, 1909 K Street, N.W., Washington, D.C. 20006. Please remit $1.00 in advance for the microfiche.

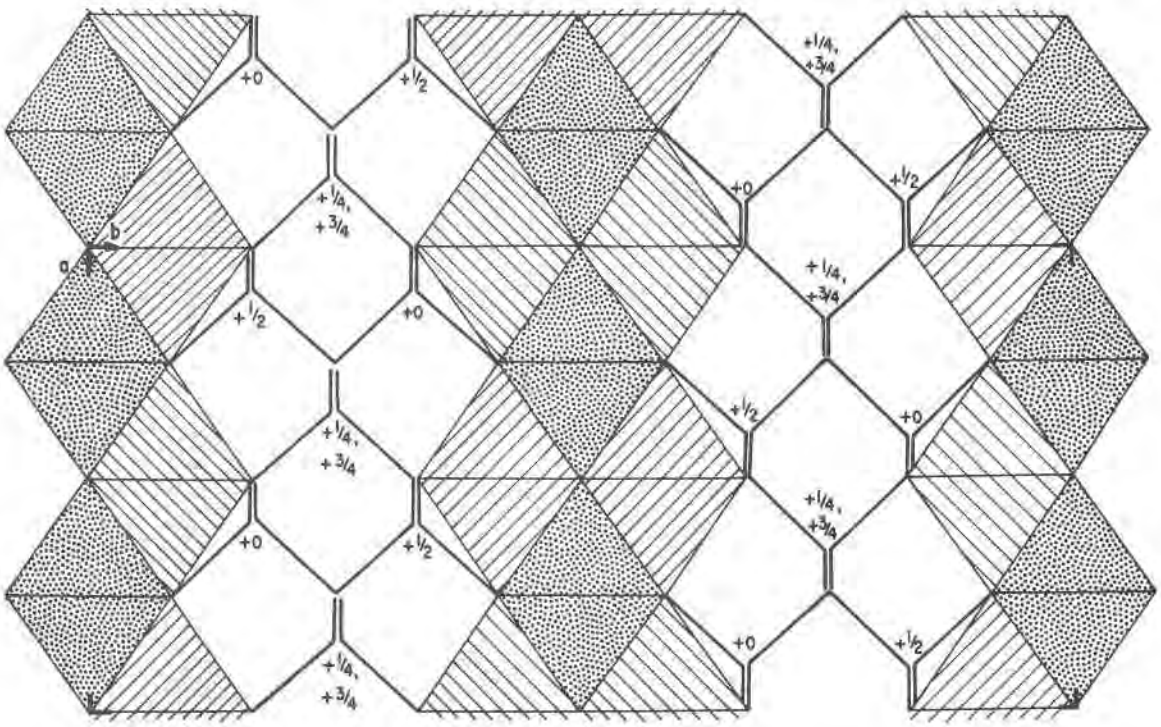

Fig. 2 Idealized polyhedral and spoke diagram for gerstmannite down [001]. The central Mg–O octahedra are stippled and form an edge-sharing chain parallel to [001]. The lateral Mn–O octahedra are populated at $z = 0$ (ruled NE–SW) and $z = ½$ (ruled NW–SE). The tetrahedra, drawn as T–O spokes, are located at $z = 0$ and $z = ½$ (Si); and $z = 1/4$, $3/4$ (Zn).

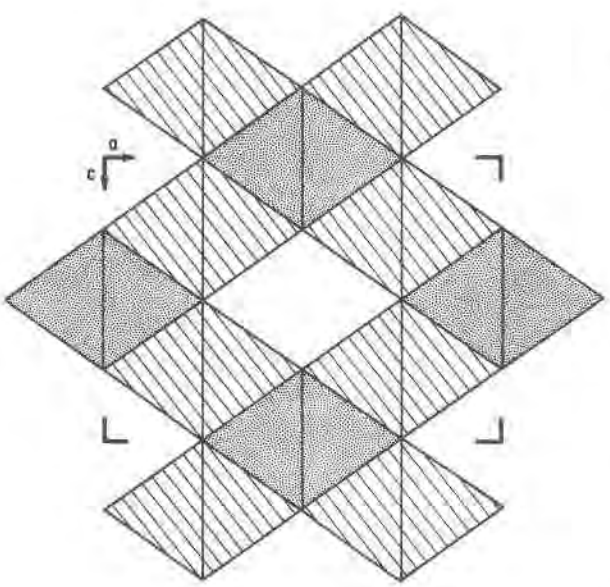

Fig. 3a. An idealized octahedral sheet of gerstmannite structure down [010]. The Mg–O octahedra are ruled and form the basis for the sheet. The Mn–O octahedra are stippled and share edges with the Mg–O octahedra both above and below the plane.

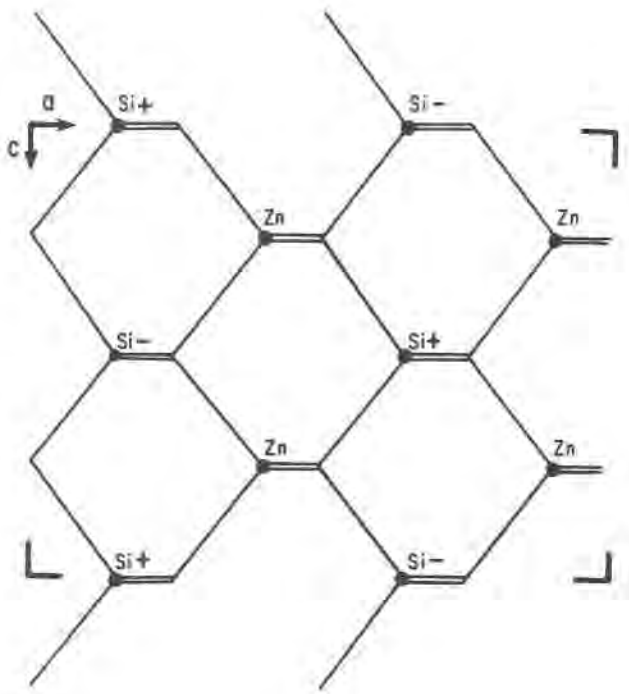

Fig. 3b. An idealized tetrahedral sheet of gerstmannite structure down [010]. The Zn–O tetrahedra are in the plane and the Si–O tetrahedra are alternately above and below the plane. Note that the Zn–O tetrahedra form corner-linked chains parallel to [001].

Table 7. Gerstmannite. Polyhedral interatomic distances and angles†

Mn			
1 Mn	-OH(2)	2.090(4)	
2	- O(3)	2.119(3)	
1	- O(1)^{iii}	2.167(4)	
2	-OH(1)	2.372(3)	
average		2.206	
			O–Mn–O′(°)
1 OH(1)	-OH(1)^{i}	2.726(7)*	70.1(1)
2 OH(1)	-OH(2)	2.779(4)*	76.7(1)
2 OH(1)	- O(1)^{iii}	2.880(4)*	78.6(1)
2 OH(1)	- O(3)	3.076(4)	86.2(1)
2 OH(2)	- O(3)	3.091(4)	94.5(1)
2 O(3)	- O(1)^{iii}	3.311(4)	101.1(1)
1 O(3)	- O(3)^{i}	3.613(5)	117.0(2)
average		3.051	88.4
Zn			
2 Zn	- O(2)	1.938(2)	
2	- O(3)^{iii}	1.957(3)	
average		1.948	
			O–Zn–O′(°)
2 O(2)	-O(3)^{iii}	2.948(4)	98.4(1)
2 O(2)	-O(3)^{iv}	3.275(4)	114.5(1)
1 O(3)^{iv}	-O(3)^{iii}	3.292(4)	114.6(1)
1 O(2)	-O(2)^{ii}	3.313(4)	117.5(2)
average		3.175	109.6
Mg			
2 Mg	-OH(2)	2.030(2)	
2	-OH(1)	2.056(2)	
2	- O(1)	2.155(3)	
average		2.080	
			O–Mg–O′(°)
2 O(1)	-OH(2)^{v}	2.777(4)*	83.1(1)
2 OH(1)	-OH(2)	2.779(4)*	85.7(1)
2 O(1)	-OH(1)^{iii}	2.880(4)*	86.3(1)
2 OH(2)	-OH(1)^{iii}	2.996(4)	94.3(1)
2 OH(1)	- O(1)	3.075(4)	93.7(1)
2 O(1)	-OH(2)	3.134(4)	96.9(1)
average		2.940	90.0
Si			
2 Si	- O(3)	1.629(3)	
1	- O(1)	1.633(3)	
1	- O(2)	1.652(3)	
average		1.636	
			O–Si–O′(°)
1 O(3)	- O(3)^{i}	2.643(5)	108.4(2)
1 O(1)	- O(2)	2.645(4)	107.2(2)
2 O(2)	- O(3)	2.653(4)	107.9(1)
2 O(1)	- O(3)	2.714(4)	112.6(1)
average		2.670	109.4

†Estimated standard errors refer to the last digit and were computed from errors in cell parameters and atomic coordinates. Equivalent positions, which refer to Table 3, include i = x, y, -z; ii = x, ½-y, ½-z; iii = ½+x, y, ½-z; iv = ½+x, ½-y, z; and v = ½-x, -y, ½-z.

*Shared octahedral edges.

Gerstmannite is yet another example of a structure type based on populations of octahedra in anion cubic close-packing and is most easily visualized as a projection down [110] direction of the NaCl structure. It is allied to a growing list of structure types such as staurolite, kyanite, spinel, $Mg_4O[Si_2O_7]$, manganostibite, and more recently $Ni_{10.3}Al_{11.4}Si_{2.3}O_{32}$–I, the last reported by Ma *et al.* (1975). All of these structures involve one axis which is some integral multiple of twice the octahedral *M*–O distance, a second axis which is some integral multiple of an octahedral edge, and a third which is also a multiple of an octahedral edge. The simplest unit for oxygen cubic close-packing has metrical properties ($m \times 4.2$Å, $n \times 3.0$Å, $p \times 3.0$Å). For gerstmannite and manganostibite, $m = 2$, $n = 6$, and $p = 2$. In addition, the units contain $2mnp$ anions. Crystals which fulfill these criteria should be examined in more detail for they may indeed represent cubic close-packing. One complex example may be holdenite, *ca.* $16Mn_3(OH)_5[Zn_2O(AsO_4)]$, *a* 8.58, *b* 31.15, *c* 11.97, *Bmcm* (Prewitt-Hopkins, 1949). Here $m = 2$, $n = 10$, $p = 4$, suggesting yet another example of an exotic population of octahedral and tetrahedral cations in an oxide cubic close-packed environment.

Table 8. Gerstmannite. Electrostatic valence balance of cations and anions*

Anion	Coordinating Cations	px	ΔMn–O	ΔMg–O	ΔZn–O	ΔSi–O
O(1)	Mn+2Mg+Si	2.00	-0.04	+0.07	-	+0.00
O(2)	2Zn+Si	2.00	-	-	-0.01	+0.02
O(3)	Mn+Zn+Si+½Ha	1.92	-0.09	-0.09	+0.01	-0.01
OH(1)	2Mn+2Mg+Hd+Ha	2.33	+0.17	-0.02	-	-
OH(2)	Mn+2Mg+Hd	1.83	-0.12	-0.05	-	-

*ΔMn–O etc., refer to differences between the individual bond distances and the polyhedral averages. Hd = hydrogen bond donor, Ha = hydrogen bond acceptor, px = sum of electrostatic bond strengths.

Bond distances and angles

Bond distances and angles are given in Table 7. The average bond distances are $^{[6]}Mn\text{–}^{[3.5]}O$ = 2.21Å, $^{[6]}Mg\text{–}^{[3.7]}O$ = 2.08Å, $^{[4]}Zn\text{–}^{[3]}O$ = 1.95Å, and $^{[4]}Si\text{–}^{[3.3]}O$ = 1.64Å (where the left superscript gives the average coordination number). These are all within 0.02Å of the distances estimated from the tables of effective ionic radii (Shannon and Prewitt, 1969). Since about 20 percent Mg substitutes for Mn^{2+} in gerstmannite, it is predicted that the Mn–O distance should be 2.17Å. It is noted that

2Mn–OH(1) = 2.37Å is an unusually long distance, a result of the combined effect of repulsion of the Mn cations away from this anion owing to the shared edge and the net electrostatic oversaturation of OH(1) by cations. This effect is reminiscent of the one reported by Moore and Araki (1975) for the crystal structures of wightmanite and gageite, where certain local cationic arrangements about an anion lead to observed distance averages longer than those predicted.

The MnO_6 octahedron shares five of its edges, four with MgO_6 and one with a symmetry equivalent MnO_6. The MgO_6 octahedron shares six edges, two with equivalent MgO_6 and four with MnO_6. All these distances are the shortest for their polyhedra, as inspection of Table 7 will show. Owing to the rather uneven distribution of shared edges for the MnO_6 octahedron, the angle distortions are considerable, ranging from 70° to 117°. The widest angle (and longest edge distance) refers to $O(3)$–$O(3)^i$ which is the edge opposite to the five shared edges. The angular distortion of the MgO_6 octahedron is much less, ranging from 83° to 97°. This arises from the smaller radius of Mg^{2+} and more balanced distribution of shared edges which are related pairwise by an inversion center.

Hydrogen bonds and electrostatic bond strengths

Symmetry and steric restrictions limit the possible hydrogen bond acceptors. OH(1), which is situated on the two-fold rotor parallel to the *c* axis, is shielded by MgO_6 octahedral edges and consequently can only bond to the equivalent OH(1) related by the mirror plane. Thus, $OH(1)\cdots OH(1)^i$ = 3.53(1)Å, is a very weak bond. OH(2), which is on the mirror plane, is further shielded by MgO_6 and MnO_6 octahedral edges. It bonds to $O(3)^{iii}$, which accordingly receives an average of one-half a bond owing to its general position. Thus, $OH(2)\cdots O(3)^{iii}$ = 3.162(5)Å, with the hydrogen on the mirror plane.

These assignments allow a complete list of electrostatic bond strength sums of cations coordinated to each of the anions (Table 8). Deviations in individual bond distances from the polyhedral averages closely follow the deviations from neutrality. Net deviations in bond distances to the coordinated cations for O(1) and O(2) are very nearly balanced since these anions are electrostatically balanced. Slightly undersaturated O(3) exhibits net shortening of bonds, and for the more severely undersaturated OH(2), this effect is more pronounced. OH(1), which is the only oversaturated anion, reveals an unusually long Mn–OH(1) distance of 2.372Å.

Acknowledgments

We thank the National Science Foundation for continued support through the grants NSF GA-40543 (Geochemistry) and through the Materials Research Laboratory grant administered to The University of Chicago.

Electron probe analysis by Dr. A. J. Irving, wet chemical analysis by Dr. Jun Ito and assistance in the optical study by Mr. A. R. Kampf are also appreciated.

References

Burnham C. W. (1966) Computation of absorption corrections, and the significance of the end effect. *Am. Mineral, 51,* 159–167.

Cromer, D. T. and D. Liberman (1970) *Los Alamos Scientific Laboratory, Univ. of Calif. Rep. LA-4403, UC-34.*

——— and J. B. Mann (1968) X-ray scattering factors computed from numerical Hartree-Fock wave-functions. *Acta Crystallogr., A24,* 321–324.

Finger, L. W. (1968) Determination of cation distribution by least-squares refinement of single crystal x-ray data. *Carnegie Inst. Wash. Year Book, 67,* 216–217.

Larsen, E. S. and H. Berman (1934) The microscopic determination of the nonopaque minerals. *U.S. Geol. Surv. Bull., 848.*

Ma, C.-B., K. Sahl and E. Tillmanns (1975) Nickel aluminosilicate, phase I. *Acta Crystallogr., B31,* 2137–2139.

Moore, P. B. and T. Araki (1974) Pinakiolite, warwickite, and wightmanite: crystal chemistry of complex 3Å wallpaper structures. *Am. Mineral., 59,* 985–1004.

——— and J. V. Smith (1970) Crystal structure of β–Mg_2SiO_4: crystal-chemical and geophysical implications. *Phys. Earth Planet. Inter., 3,* 166–177.

Prewitt-Hopkins, J. (1949) X-ray study of holdenite, mooreite and torreyite. *Am. Mineral., 34,* 589–595.

Ramachandran, G. N. and R. Srinivasan (1970) *Fourier Methods in Crystallography.* Wiley-Interscience, New York, 96–119.

Shannon, R. D. and C. T. Prewitt (1969) Effective ionic radii in oxides and fluorides. *Acta Crystallogr., B25,* 925–946.

Zachariasen, W. H. (1968) Experimental tests of the general formula for the integrated intensity of a real crystal. *Acta Crystallogr., A24,* 212–214.

Manuscript received, February 5, 1976; accepted for publication, June 29, 1976.